Influence of hydrogen charging parameters on the strength of 60S2A steel

M. M. Hvozdiuk · T. V. Hembara · S. T. Shtayura · M. V. Hrynenko · P. M. Hrytsyshyn

Received: 16 April 2025 / Revised: 4 July 2025 / Accepted: 1 October 2025

Abstract
Tensile tests of the alloyed 60S2A spring steel were carried out under the action of gaseous hydrogen with increased parameters: temperature 400 °C, and pressure 6 MPa. The true fracture diagrams of 60S2A steel were plotted for different hydrogen charging times. The optical-digital image correlation method of the sample surface and special software were used to determine the value of local deformation. It was established that fracture stresses and strains decrease linearly with increasing hydrogenation time.

Keywords 60S2A steel · Hydrogen environment · True stress · True strain · Hydrogen embrittlement index · Digital image correlation

Introduction

Determination of the hydrogen influence on strength characteristics of structural materials, especially in environments with an increased hydrogen content (fuel systems, thermal power engineering, chemical industry, and hydrogen power engineering), is one of the current problems of materials science [1–4]. The 60S2A steel is alloyed with spring steel with improved mechanical properties (Table 1). Microcracks are formed, the yield strength and ultimate strain decrease; however, under the action of high temperature and hydrogen pressure (for example, at 400 °C and 6 MPa) [3]. The time to fracture can be significantly reduced, and the allowable load can be reduced even with a small amount of hydrogen accumulated in the steel matrix [5, 6]. Therefore, it is important to establish the invariant characteristics of the material and their change, taking into account the influence of the hydrogen environment under operational parameters.

The purpose of this investigation is to study the exposure time of the hydrogen environment influence on the true destructive stresses and strains in 60S2A steel using a high-precision modern non-contact optical-digital image correlation method, which makes it possible to control displacement in the local zone with an appropriate mathematical software processing and plotting of fracture diagrams.

Translated from *Fizyko-Khimichna Mekhanika Materialiv*, Vol. 61, No. 5, pp. 97–101, September–October, 2025. Ukrainian
DOI: https://doi.org/10.15407/pcmm2025.05.097

Table 1 Application of the 60S2A steel (analog of 9260 steel) in Hydrogen [7–9]

Application	Device (component)	Environmental conditions	Potential risks	Measures to protect steel
Hydrogen compressors	High load springs	Hydrogen under pressure up to 20 MPa, $T<100$ °C	Hydrogen embrittlement	Hardening and tempering; coatings with Ni and Zn
Hydrogen cars (H_2 fuel cell)	Spring elements, bumpers	Periodical contact with hydrogen	Slow hydrogen degradation	Heat treatment, microstructure control
Hydrogen system fittings	Valve springs, seals	Hydrogen environment, $T<350$ °C	High pressure and temperature	Alloying with Cr and Si
Hydrogen-powered railway equipment	Springs of hydrogen locomotives	Influence of atmospheric hydrogen	Cumulative embrittlement during vibrations	Surface treatment, protective layers

Material, equipment, and research methods

The influence of the hydrogen charging time on the strength characteristics of steel 60S2A, which contains [mass%]: 0.58–0.63 C, 1.6–2.0 Si, 0.6–0.9 Mn, 0.25 Ni, 0.025 S, 0.025 P, 0.3 Cr, and 0.2 Cu (GOST 14959-79), was studied. Carbon provides high strength, silicon provides elasticity and tensile strength, and manganese improves the steel's weldability and wear resistance. This steel is used in mechanical engineering for the production of various high-strength and deformation-resistant spring elements.

Twenty cylindrical samples, five each for different hydrogen charging parameters, were tested (Fig. 1). The non-contact optical-digital system (ODS) and a digital image correlation (DIC) algorithm were used to plot the true deformation diagrams, taking into account the hydrogen influence. The optical-digital image correlation method [10, 11] was used to measure true strains in the working zone of the sample, where the stress-strain state is homogeneous. The local deformation, its distribution over the entire surface of the sample, and the place of the fracture beginning were determined in this way.

The prepared samples were hydrogenated from the gaseous phase in a sealed stainless steel chamber at 400 °C, and a pressure of 6 MPa for 24, 48, and 96 h. After that, a black paint base was applied to the specially prepared working surface of the sample. Then, the white paint in the form of stochastic dot pattern was sprayed onto this black paint base (Fig. 2). The sample was fixed in the grips of an electromechanical breaking machine FP-100, and loaded with tension, simultaneously registering the loading force with an inductive standard dynamometer until fracture (Fig. 3). The movable traverse of the machine displacement speed was 1 mm/min. The elongation of the sample's central working zone was remotely recorded using a digital camera in parallel. The results were processed using Power Graph 3.3.8 [11].

The strength characteristics of the steel were found from the true fracture diagrams P–Δl, where P is the force, and Δl is the elongation of the sample material in the zone of maximum deformations. The true stresses S_i were calculated from the $S_i = P_i/F_i$ ratio, where F_i is the real cross-sectional area considering the change in its diameter. The true deformation e in the local volume was determined from the results of two-directional displacement on a 1 mm base using an optical-digital speckle image correlator.

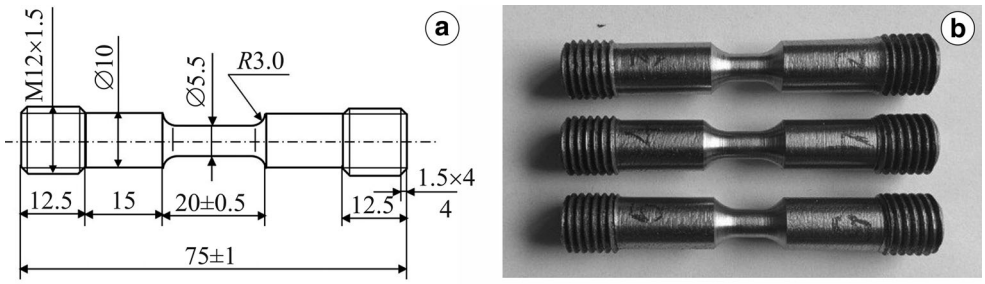

Fig. 1 Scheme **a** and **b** photos of the experimental samples

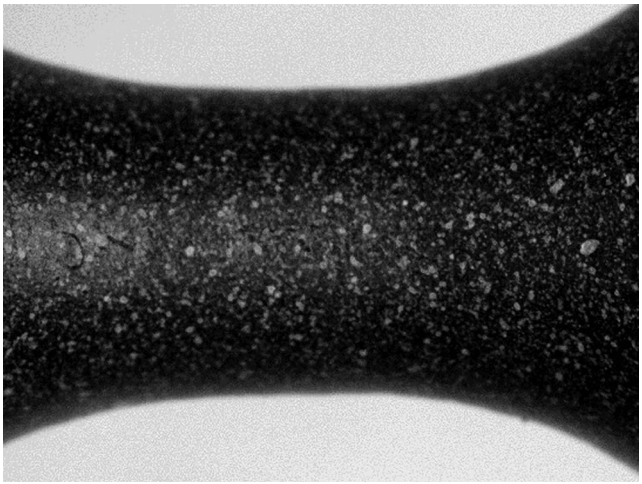

Fig. 2 Photo of the surface of the sample prepared for the experiment

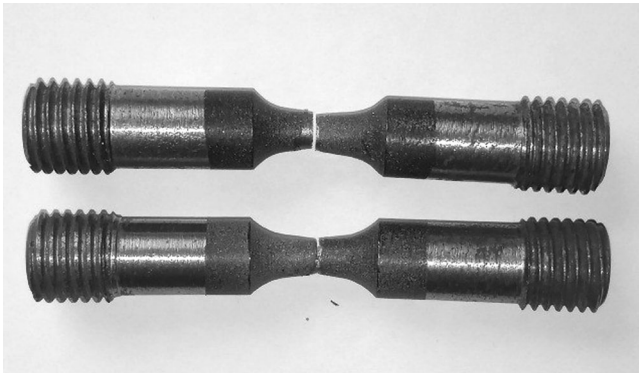

Fig. 3 Fractured samples

Results and analysis

The dependence of the hydrogen charging time influence on the relative reduction area of the material Ψ was obtained (Fig. 5a) from the true fracture diagrams of the samples in the *S*–*e* range for different hydrogen charging times (Fig. 4).

The influence of hydrogen in the elastic zone of deformation was not revealed. With increasing hydrogen charging time and therefore hydrogen concentration, fracture stresses decrease (Fig. 5b), and deformations (Fig. 6a) were recorded, practically according to the linear law. The true fracture stress decreased by 12%, and fracture deformation by 18% at maximum hydrogenation, compared to the material in the initial state.

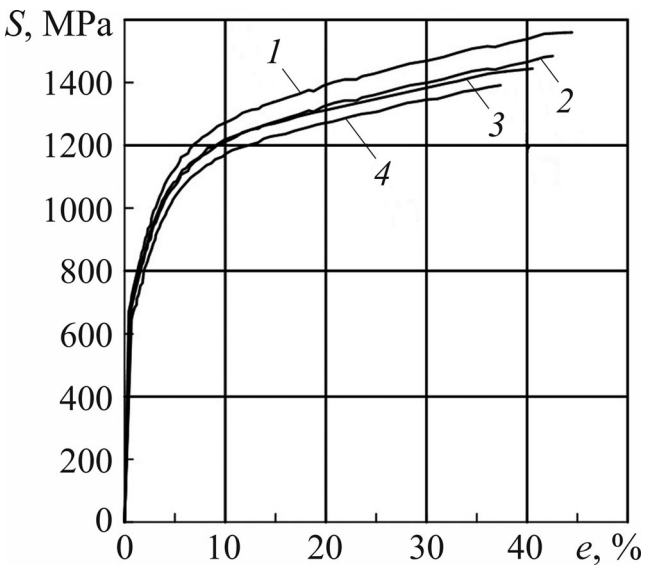

Fig. 4 True fracture diagrams of samples for different hydrogen charging time: (*1*) is the initial state, (*2*) 24 h of hydrogen charging, (*3*) 48 h, (*4*) 96 h

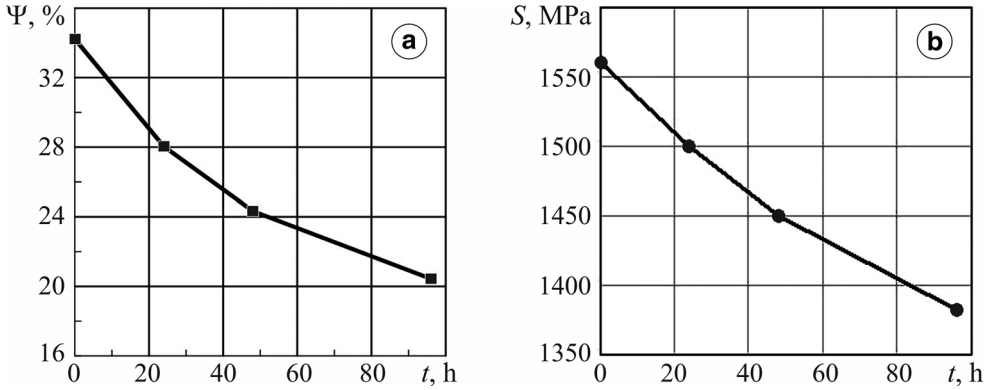

Fig. 5 Influence of hydrogen charging time on **a** the relative reduction and **b** destructive stresses of the sample

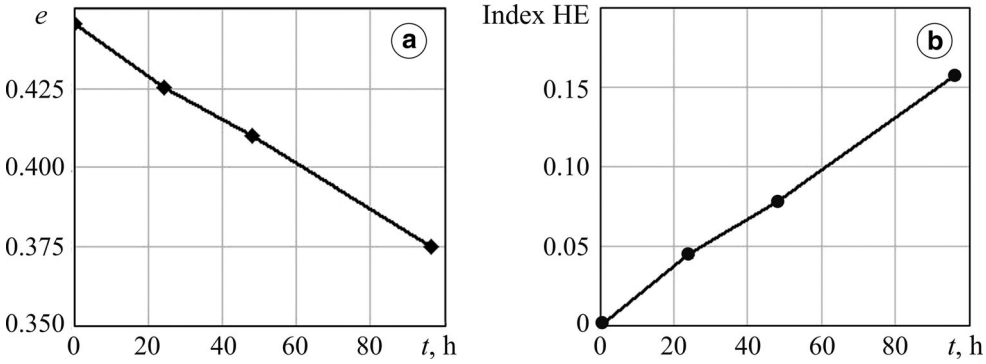

Fig. 6 Influence of hydrogen charging time on **a** the fracture deformation of samples and **b** the hydrogen embrittlement index

The 60SA steel's resistance to hydrogen embrittlement was evaluated by the index HE, which was determined from the ratio

$$\text{Index HE} = \frac{e_0 - e_\text{H}}{e_0}.$$

This index increases with hydrogen charging time (Fig. 6b), indicating the steel's sensitivity to hydrogen degradation, which increases with process duration, reaching 15.7% after 96 h. The metal under such conditions fractures brittlely, with no visible signs of plastic deformation.

Conclusions

The negative influence of absorbed hydrogen on the strength and plasticity of 60S2A steel was established. This influence changes with the increase in hydrogen charging time at constant temperature and pressure according to the linear law. The fracture stresses decrease by an average of 12%, and the relative ultimate tensile strength decreases by 18% after 96 h of exposure of samples to gaseous hydrogen at 400 °C, and pressure of 6 MPa. This result can be extended to 9260 (USA), SUP6 (Japan), and 60MnSiCr4 (Germany) analogues of this steel to guarantee the service life of structural elements.

Funding All authors declare that no funds, grants, or other support were received during the preparation of this manuscript.

Author Contribution All authors contributed equally to the work and read and approved the final manuscript.

Data availability The datasets generated and/or analyzed in the current study are available from the corresponding author upon reasonable request.

Conflict of interest All authors declare that they have no potential conflict of interest in relation to the study in this paper. All authors have no relevant financial or non-financial interests to disclose.

References

1. Y. Ivanytskyi, Y. Kharchenko, O. Hembara, O. Chepil, Y. Sapuzhak, N. Hembara, The energy approach to the evaluation of hydrogen effect on the damage accumulation. Procedia Structural Integrity **16**, 126–133 (2019). https://doi.org/10.1016/j.prostr.2019.07.031
2. Q. Jiang, O.V. Hembara, O.Y. Chepil, Modeling of the influence of hydrogen on the accumulation of defects in steels under high-temperature creep. Mater. Sci **55**, 251–259 (2019). https://doi.org/10.1007/s11003-019-00296-x
3. M. Dutkiewicz, O. Hembara, Y. Ivanytskyi, M. Hvozdiuk, O. Chepil, M. Hrynenko, N. Hembara, Influence of hydrogen on the fracture resistance of pre-strained steam generator steel 22K. Materials **15**, 6596 (2022). https://doi.org/10.3390/ma15196596
4. M. Dutkiewicz, O. Hembara, O. Chepil, M. Hrynenko, T. Hembara, A new energy approach to predicting fracture resistance in metals. Materials **16**, 1566 (2023). https://doi.org/10.3390/ma16041566
5. I.M. Dmytrakh, A.M. Syrotyuk, O.P. Krasiuk, P.A. Bolkot, O.T. Tsyrulnyk, R.L. Leshchak, V.M. Malyuk, O.V. Brychynskyy, Specific features of hydrogen-charged 60S2A steel fragmentation under static explosion tests. Mater. Sci **60**, 543–548 (2025). https://doi.org/10.1007/s11003-025-00917-8
6. I.M. Dmytrakh, A.M. Syrotyuk, O.T. Tsyrulnyk, Influence of electrochemical hydrogen charging on loss of plasticity and development of volumetric microdamaging of 60S2A steel. Mater. Sci **60**, 148–155 (2024). https://doi.org/10.1007/s11003-025-00865-3
7. S.P. Lynch, Hydrogen embrittlement phenomena and mechanisms. Corros. Rev **30**, 105–123 (2012). https://doi.org/10.1515/corrrev-2012-0502
8. F. Liu, Y. Liu, X. Li, S. Zhao, H. , Fang, Hydrogen embrittlement behavior of a high-strength spring steel treated by Q&P process. J Mater Eng Perform **33**, 4287–4296 (2024). https://doi.org/10.1007/s11665-024-09242-8
9. H.J. Wan, X.Q. Wu, H.L. Ming, J.Q. Wang, E.H. Han, Effects of hydrogen charging time and pressure on the hydrogen embrittlement susceptibility of X52 pipeline steel material. Acta Metall. Sin. (Engl. Lett.) **37**, 293–307 (2024). https://doi.org/10.1007/s40195-023-01625-5
10. Y. Ivanyts'kyi, O. Hembara, W. Dudda, V. Boyko, S. Shtayura, Combined FEM and DIC techniques for the 2D analysis of the stress–strain fields and hydrogen diffusion near a blunt crack tip. Strength Mater **54**, 256–266 (2022). https://doi.org/10.1007/s11223-022-00399-y
11. Ya L. Ivanyts'kyi, Yu V. Mol'kov, P.S. Kun', T.M. Lenkovs'kyi, M. Wójtowicz, Determination of the local strains near stress concentrators by the digital image correlation technique. Mater Sci **50**, 488–495 (2015). https://doi.org/10.1007/s11003-015-9746-7

Authors and Affiliations

M. M. Hvozdiuk[1,2] · T. V. Hembara[3] · S. T. Shtayura[1] · M. V. Hrynenko[1] · P. M. Hrytsyshyn[4]

✉ M. M. Hvozdiuk
hvozdjuk@gmail.com

T. V. Hembara
taras.gembara@gmail.com

S. T. Shtayura
stepan.shtayura@gmail.com

M. V. Hrynenko
mykhailogrynenko@gmail.com

P. M. Hrytsyshyn
p.hrytsyshyn@gmail.com

[1] Karpenko Physico-Mechanical Institute, National Academy of Sciences of Ukraine, Lviv, Ukraine

[2] Lviv Polytechnic National University, Lviv, Ukraine

[3] Lviv State University of Life Safety, Lviv, Ukraine

[4] Lviv Scientific-Research Institute of Forensic Expertise, Lviv, Ukraine